# Involvement of Ca2+-ATPase in suppressing the appearance of bovine helically motile spermatozoa with intense force prior to cryopreservation

Duritahala

Sakase, Mitsuhiro

Harayama, Hiroshi

# Original Article

# Involvement of Ca²⁺-ATPase in suppressing the appearance of bovine helically motile spermatozoa with intense force prior to cryopreservation

## DURITAHALA[1)], Mitsuhiro SAKASE[2)] and Hiroshi HARAYAMA[1, 3)]

[1)]*Laboratory of Reproductive Biology, Division of Animal Science, Department of Bioresource Science, Graduate School of Agricultural Science, Kobe University, Kobe 657-8501, Japan*
[2)]*Hokubu Agricultural Technology Institute, Hyogo Prefectural Technology Center for Agriculture, Forestry and Fisheries, Hyogo 669-5254, Japan*
[3)]*Biosignal Research Center, Kobe University, Kobe 657-8501, Japan*

**Abstract.** In cattle, cryopreserved spermatozoa are generally used for artificial insemination (AI). Many of these specimens exhibit helical movement, although the molecular mechanisms underlying this phenomenon remain unclear. This study aimed to characterize helically motile spermatozoa, investigate the involvement of Ca²⁺-ATPase in suppressing the appearance of these spermatozoa prior to cryopreservation, and examine the potential of helical movement as an index of sperm quality. In the cryopreserved semen, approximately 50% of spermatozoa were helically motile, whereas approximately 25% were planarly motile. The helically motile samples swam significantly faster than those with planar movement, in both non-viscous medium and viscous medium containing polyvinylpyrrolidone. In contrast, in non-cryopreserved semen, planarly motile spermatozoa outnumbered those that were helically motile. Fluorescence microscopy with Fluo-3/AM and propidium iodide showed that flagellar $[Ca^{2+}]_i$ was significantly higher in cryopreserved live spermatozoa than in non-cryopreserved live ones. The percentage of non-cryopreserved helically motile spermatozoa was approximately 25% after washing, and this increased significantly to approximately 50% after treatment with an inhibitor of sarcoplasmic reticulum Ca²⁺-ATPases (SERCAs), "thapsigargin." Immunostaining showed the presence of SERCAs in sperm necks. Additionally, the percentages of cryopreserved helically motile spermatozoa showed large inter-bull differences and a significantly positive correlation with post-AI conception rates, indicating that helical movement has the potential to serve as a predictor of the fertilizing ability of these spermatozoa. These results suggest that SERCAs in the neck suppress the cytoplasmic Ca²⁺-dependent appearance of helically motile spermatozoa with intense force in semen prior to cryopreservation.
Key words: Artificial insemination, Cryopreservation, Motility assessment, Sarcoplasmic reticulum Ca²⁺-ATPase (SERCA), Semen

**(J. Reprod. Dev. 68:** 181–189, 2022)

**S**perm motility is conventionally believed to be an essential characteristic for determining semen quality and estimating male reproductive performance. In cattle artificial insemination (AI) centers, sperm motility is routinely investigated immediately after collection, during the handling process before cryopreservation, and after cryopreservation by subjective microscopy and supplementally by two-dimensional (2D) computer-assisted sperm analysis (CASA) [1, 2]. In these assessments of sperm motility, the linearity and velocity of movement are considered important parameters. In other words, the qualities of fresh ejaculates and cryopreserved semen are evaluated on the basis of the percentage of spermatozoa that exhibit rapid and progressive movement. Thus, cryopreserved semen, which are allowed for AI programs, include an abundance of spermatozoa that exhibit rapid and progressive movement. Despite multiple examinations of sperm motility, the results of AI still vary widely among different semen suppliers. Therefore, new criteria for assessing bovine sperm motility have emerged. We recently conducted studies to improve

methods of evaluating sperm flagellum functions using new criteria for helical movement with three-dimensional (3D) rotation [3] and 3D full-type hyperactivation [4, 5]. The results of these studies indicated that the precise evaluation of these 3D movements requires a detailed investigation of the motility patterns of each spermatozoon in a chamber with sufficient depth (50 µm) under a microscope with relatively high magnification (× 40 objective lens). Although CASA systems are often used in current research, CASA motility parameters are obtained by the analyses of 2D trajectories of motion using videos of sperm movement, which are usually captured in a chamber with insufficient depth for 3D movement (10–20 µm) under a microscope with low magnification (× 10–20 objective lens). Thus, it is difficult to evaluate 3D sperm movements (helical movements with 3D rotation and 3D full-type hyperactivation) precisely using the current CASA systems. Research groups are working to develop new CASA systems to investigate the 3D movements that spermatozoa can exhibit freely in a chamber with sufficient depth [6–8].

According to previous observations [3, 9], bovine spermatozoa exhibit two patterns of vigorous movement. Cryopreserved semen abound with vigorously motile spermatozoa with helical movement, whereas vigorously motile spermatozoa of non-cryopreserved semen tend to exhibit 2D planar movement, although the cause of these different patterns is unclear. Bailey *et al.* reported that the cytoplasmic Ca²⁺ level of cryopreserved bovine spermatozoa was significantly higher than that of non-cryopreserved spermatozoa [10–13]. They also suggested that this cryopreservation-induced increase in the cy-

Correspondence: Duritahala (e-mail: duritahala@gmail.com) and H Harayama (e-mail: harayama@kobe-u.ac.jp)

toplasmic $Ca^{2+}$ level is an initiator of capacitation (cryo-capacitation), leading to the occurrence of a precocious acrosome reaction in the sperm head [11–13]. Several molecules maintain intracellular $Ca^{2+}$ homeostasis in both spermatozoa and somatic cells. Among the modulators of the cytoplasmic $Ca^{2+}$ level, the sarcoplasmic reticulum $Ca^{2+}$-ATPase (SERCA) is an important member of the cytoplasmic $Ca^{2+}$ clearance system [14, 15]. This study aimed to characterize bovine helically motile spermatozoa, investigate the involvement of SERCAs in suppressing the appearance of these spermatozoa before cryopreservation, and examine the potential of helical movement to serve as an index of sperm quality.

## Materials and Methods

### Reagents and sperm samples

All reagents were purchased from FUJIFILM Wako Pure Chemical Corporation (Osaka, Japan), unless specified otherwise.

The bovine samples were used with the permission of the Hokubu Agricultural Technology Institute, Hyogo Prefectural Technology Center for Agriculture, Forestry and Fisheries (Hokubu Institute) under the research project plan "Improvement of Fertility Assay for Japanese Black Bull Spermatozoa (2016–2021)". Fresh ejaculates were obtained for the routine investigation of semen characteristics to evaluate male reproductive performance, as described previously, with minor modifications [3, 4, 16]. In brief, an artificial vagina was used to collect the ejaculates from 10 sire candidates (Japanese Black bulls, > 1-year-old), which were fed at the Hokubu Institute. Aliquots of freshly ejaculated samples were used for the subjective observation of sperm motility under light microscope. The remaining samples with good quality were transported to our laboratory at Kobe University within 2.5 h at approximately 25–30°C. After routine investigation of semen characteristics, surpluses of the samples were used as the non-cryopreserved semen in this study. The straws of the cryopreserved semen of the sires and sire candidates (approximately $1.0 \times 10^8$ cells/ml) were provided by Hokubu Institute.

These samples were gently diluted with PBS containing 0.1% polyvinyl alcohol (PVA, average molecular weight 30,000–70,000, Cat. # P8136, Sigma-Aldrich Co., St Louis, MO, USA) (PBS-PVA) or PBS containing 1 or 2.5% polyvinylpyrrolidone (PVP, average molecular weight 360,000, Cat. # PVP360, Sigma-Aldrich) (PBS-PVP) to adjust the sperm concentration to $2.5 \times 10^7$ spermatozoa/ml. Seminal plasma or semen extender was removed from the samples in some experiments, including the detection of cytoplasmic $Ca^{2+}$ in the sperm flagella with Fluo-3/AM, treatment with thapsigargin and $CaCl_2$, Western blotting, and indirect immunofluorescence. In these cases, the spermatozoa were washed in PBS-PVA by centrifugation at 700 *g* for 5 min. In the preliminary experiments, an increase in washing time tended to induce small head-to-head agglutination among several cryopreserved spermatozoa, although this tendency was rarely observed for non-cryopreserved spermatozoa (data not shown). As sperm agglutination made it difficult to determine the motility pattern of each spermatozoon, cryopreserved and non-cryopreserved spermatozoa were washed once and three times, respectively.

### Evaluation of sperm motility

To capture movies of the motility patterns of spermatozoa [3, 4], an aliquot (10 µl) of the diluted semen or a suspension (10 µl) of washed spermatozoa was placed in a chamber with a depth of 50 µm (Fujihira Industry, Tokyo, Japan) on a warmed stage (38.5ºC) of an upright microscope (Olympus Corporation, Tokyo, Japan). Microscopic movies of the spermatozoa were captured using a CMOS camera (BU238M, Toshiba Teli, Tokyo, Japan) with × 40 objective lenses at a frame rate of 100 Hz and were recorded as non-compressed movies (FCR-1, TechnoScope, Saitama, Japan). These were converted into sequential frame images (JPEG images) using "Free Video to JPG Converter" software. Sperm motility patterns were classified based on the following characteristics: (i) planar movement with progressive or round movement, (ii) helical movement with progressive or round movement, (iii) only beating movement, and (iv) immobility. Sperm motility patterns in each sample were determined for approximately 100 spermatozoa using sequential images from each movie that were played back frame by frame using Windows Media Player (Microsoft, Redmond, WA, USA).

Sperm velocity was determined as previously described, with some modifications [3, 17]. Briefly, six sequential frames of the movies (every 1/100 sec; at time 0/100 sec, 1/100 sec, 2/100 sec, 3/100 sec, 4/100 sec, and 5/100 sec) were stored as sequential images in Microsoft PowerPoint 2013, Japanese Version (Microsoft). The positions (coordinates $X_{0-5}$, $Y_{0-5}$) of the central edge of the apical ridge of the sperm head were determined using PowerPoint images, as shown in Supplementary Fig. 1.

The migration length for 1/100 sec on PowerPoint images (cm) was measured in each spermatozoon according to the following numerical formula:

The migration length for 1/100 sec on the PowerPoint image (cm) = {square root $[(X_0–X_1)^2 + (Y_0–Y_1)^2]$ + square root $[(X_1–X_2)^2 + (Y_1–Y_2)^2]$ + square root $[(X_2–X_3)^2 + (Y_2–Y_3)^2]$ + square root $[(X_3–X_4)^2 + (Y_3–Y_4)^2]$ + square root $[(X_4–X_5)^2 + (Y_4–Y_5)^2]\}/5$.

The sperm velocity (µm/0.01 sec) was then calculated according to the following numerical formula:

The sperm velocity (µm/0.01 sec) = the migration length for 1/100 sec on the PowerPoint image (cm) ÷ 0.1216 (the actual migration length on the sperm chamber "1 µm" was equivalent to the migration length on the PowerPoint image of "0.1216 cm").

Indexes of the maximal flagellar bends were determined as described below. Frames of the movies (including spermatozoa exhibiting the maximal flagellar bend) were stored as images in Microsoft PowerPoint 2013. The positions (coordinates $(X_{11}, Y_{11})$ and $(X_{12}, Y_{12})$: edges of the flagellar arc exhibiting the maximal flagellar bend; $(X_{13}, Y_{13})$ and $(X_{14}, Y_{14})$: edges of the perpendicular from the peak of the arc of the maximal flagellar bend to the chord) were determined on the PowerPoint images (Supplementary Fig. 2-A). The chord length (the length between both edges of the flagellar arc exhibiting the maximal flagellar bend) and camber (the length of the perpendicular from the peak of the arc of the maximal flagellar bend to the chord) on PowerPoint images (cm) were measured for each spermatozoon according to the following numerical formula.

The chord length on the PowerPoint image (cm) = square root $[(X_{11}–X_{12})^2 + (Y_{11}–Y_{12})^2]$

The camber on the PowerPoint image (cm) = square root $[(X_{13}–X_{14})^2 + (Y_{13}–Y_{14})^2]$

The chord length and camber (µm) were then calculated according to the following numerical formula:

The chord length or camber (µm) = the chord length or camber on the PowerPoint image (cm) ÷ 0.1216 (the actual length on the sperm chamber "1 µm" was equivalent to the length on the PowerPoint image of "0.1216 cm").

### Detection of cytoplasmic $Ca^{2+}$ in sperm flagella

Cytoplasmic $Ca^{2+}$ was detected in the sperm flagella, as described previously, with several modifications [18]. Briefly, washed spermatozoa ($1.0 \times 10^8$ cells/ml) were loaded with Fluo-3/AM (Dojindo

Laboratories, Kumamoto, Japan, final concentration: 5 µM) in the presence of 0.02% Pluronic F127 (Sigma-Aldrich) for 10 min in the dark and washed. Fluo-3/AM-loaded spermatozoa ($2.5 \times 10^7$ spermatozoa/ml) were used for the detection of cytoplasmic $Ca^{2+}$ either immediately or after treatment with thapsigargin and $CaCl_2$. For detection, the cells were mixed with propidium iodide (PI, Thermo Fisher Scientific Corporation, Waltham, MA, USA, final concentration: 12 µM) and used for observation under a microscope equipped with epifluorescence (U-FBW mirror unit composed of BP460-495 excitation filter, DM505 dichroic mirror, and BA510IF emission filter, Olympus Corporation, Tokyo, Japan). All images from each experiment were taken under the same conditions and used to measure the intensity of Fluo-3/AM fluorescence in the flagellum of each live (PI-negative) spermatozoon with ImageJ software (National Institute of Health, Bethesda, MD, USA). The relative intensity of Fluo-3/AM fluorescence in the flagellum of each live spermatozoon was calculated according to the numerical formula shown in the figure legends.

### Treatment with thapsigargin and $CaCl_2$

Thapsigargin is an inhibitor of SERCAs in somatic cells and suppresses SERCA-dependent pumping of cytoplasmic $Ca^{2+}$ into internal stores. Consequent depletion of $Ca^{2+}$ in the internal stores induces the influx of extracellular $Ca^{2+}$ into the cytoplasm via the store-operated channel. As a result of these events, cytoplasmic $Ca^{2+}$ levels can be increased pharmacologically [19–21]. Mammalian spermatozoa have unique cell organelles, and the redundant nuclear envelopes of the neck and outer acrosomal membrane of the head function as internal stores instead of the endoplasmic reticulum [22, 23].

Washed non-cryopreserved spermatozoa ($2.5 \times 10^7$ spermatozoa/ ml) were treated with thapsigargin (final concentrations: 0, 5, and 10 µM, EMD Millipore Corp, Billerica, MA, USA) for 45 or 90 min in a 38.5°C water bath. Thapsigargin was dissolved in dimethyl sulfoxide (DMSO) as a stock solution (5 mM or 10 mM) and then added to the sperm suspension. DMSO was also added to equalize the final concentrations of the solvent among all samples. In this treatment, modified Krebs-Ringer HEPES medium containing glucose and antibiotics ($CaCl_2$ concentration; 1.71 mM, without bovine serum albumin and without $NaHCO_3$, the non-capacitation medium) plus 0.1% PVA (mKRH-PVA) [24] was used, because incubation for at least 45 min was required to obtain the apparent effects of thapsigargin on sperm motility patterns (see the Results section).

### Western blotting and indirect immunofluorescence

Western blotting was performed using extracts of washed spermatozoa ($3 \times 10^6$ cells/lane), 6% polyacrylamide gel, polyvinylidene difluoride membrane (Merck Millipore Co., Darmstadt, Germany), and Amersham ECL Prime Western Blotting Detection Reagent (GE Healthcare UK Limited, Buckinghamshire, UK) [25, 26]. The primary antibody was mouse anti-SERCA1/2/3 monoclonal antibody (1:100, $IgG_1$, 2 µg protein/ml, Cat. # sc-271669, Santa Cruz Biotechnology, Inc., Dallas, TX, USA). According to the datasheet from the manufacturer, this primary antibody was raised against amino acids 1-300 mapping at the N-terminus of a SERCA of human origin. Thus, we confirmed the high similarity of the amino acid sequences of SERCA1/2/3 between humans and cattle (Supplementary Table 1). In the negative control experiments, normal mouse $IgG_1$ (1:50, 2 µg protein/ml, Cat. # X0931, Dako Agilent Pathology Solutions, Santa Clara, CA, USA; 1:100, 2 µg protein/ml, Cat. # sc-3877, Santa Cruz Biotechnology) was used to confirm the reaction specificity of the

antibodies. The secondary antibody was a horseradish peroxidase-conjugated goat anti-mouse immunoglobulin polyclonal antibody (1:20,000, Cat. # P0447, Dako).

Indirect immunofluorescence was performed as described previously [26, 27] using smear preparations of washed spermatozoa ($5 \times 10^5$ cells). They were treated with 3% paraformaldehyde, 1% (vol/vol) Triton X-100 (Sigma-Aldrich), mouse anti-SERCA1/2/3 monoclonal antibody (1:10, 20 µg protein/ml), and fluorescein isothiocyanate-conjugated rabbit anti-mouse immunoglobulin polyclonal antibodies (1:100, Cat. # F0261, Dako). To confirm antibody reaction specificity, normal mouse $IgG_1$ (1:5, 20 µg protein/ml, Cat. # X0931, Dako) was used for the negative control experiments.

### Post-AI conception rates

Data on post-AI conception rates were provided by the Hokubu Institute. These rates were calculated from the results of routine AI performed at least 33 times with the cryopreserved spermatozoa of each of the 10 bulls. The AI procedures have been previously described [16].

### Statistical analyses

Statistical analyses were performed using Bell Curve for Excel (Version 3.21, Social Survey Research Information Co., Ltd., Tokyo, Japan), which is an add-in software for the Japanese version of Microsoft Excel 2016 (Microsoft). Data were statistically analyzed using the $t$-test or one-way analysis of variance (ANOVA) after arcsine transformation (in case the data did not include values above 1 (100%)) and tests for homogeneity of variance. When F-test results were significant in the ANOVA, individual means were further tested using the Tukey-Kramer test. The correlation between the post-AI conception rates and the percentages of cryopreserved spermatozoa exhibiting different movement patterns was analyzed using Spearman's rank correlation coefficient test. The level of significance was set at $P < 0.05$. All data are represented as means ± standard deviations.

## Results

### Experiment 1. Characteristics of helically motile spermatozoa

In the non-cryopreserved semen diluted with PBS-PVA, planarly motile spermatozoa (56 ± 1%) were predominantly observed, as opposed to helically motile spermatozoa (32 ± 3%). However, in the cryopreserved semen diluted with PBS-PVA, the percentages of helically motile spermatozoa (55 ± 10%) were significantly higher than those of planarly motile spermatozoa (27 ± 11%) (Fig. 1-A and Supplementary Movie 1). Although the maximal flagellar bends of helically motile spermatozoa had similar shapes and sizes to those of planarly motile spermatozoa (Fig. 1-B and Supplementary Fig. 2-B), the former swam significantly faster than the latter (Fig. 1-C). In addition, considering the viscous environment of the female reproductive tract, sperm movement patterns were observed in the cryopreserved semen diluted with the viscous medium. As shown in Fig. 1-D and Supplementary Movie 2, dilution with PBS-PVP (viscous medium containing 1% or 2.5% PVP and no PVA) significantly decreased the percentages of helically motile spermatozoa and increased the percentages of planarly motile spermatozoa, compared with the cryopreserved semen diluted with PBS-PVA (the non-viscous medium containing 0.1% PVA and no PVP). However, in the samples diluted with PBS-PVP, the remaining spermatozoa with helical movement swam significantly faster than those with planar motility (Fig. 1-E).

The seminal plasma and egg yolk-based extender included $Ca^{2+}$ that interfered with loading Fluo-3/AM into the spermatozoa. After
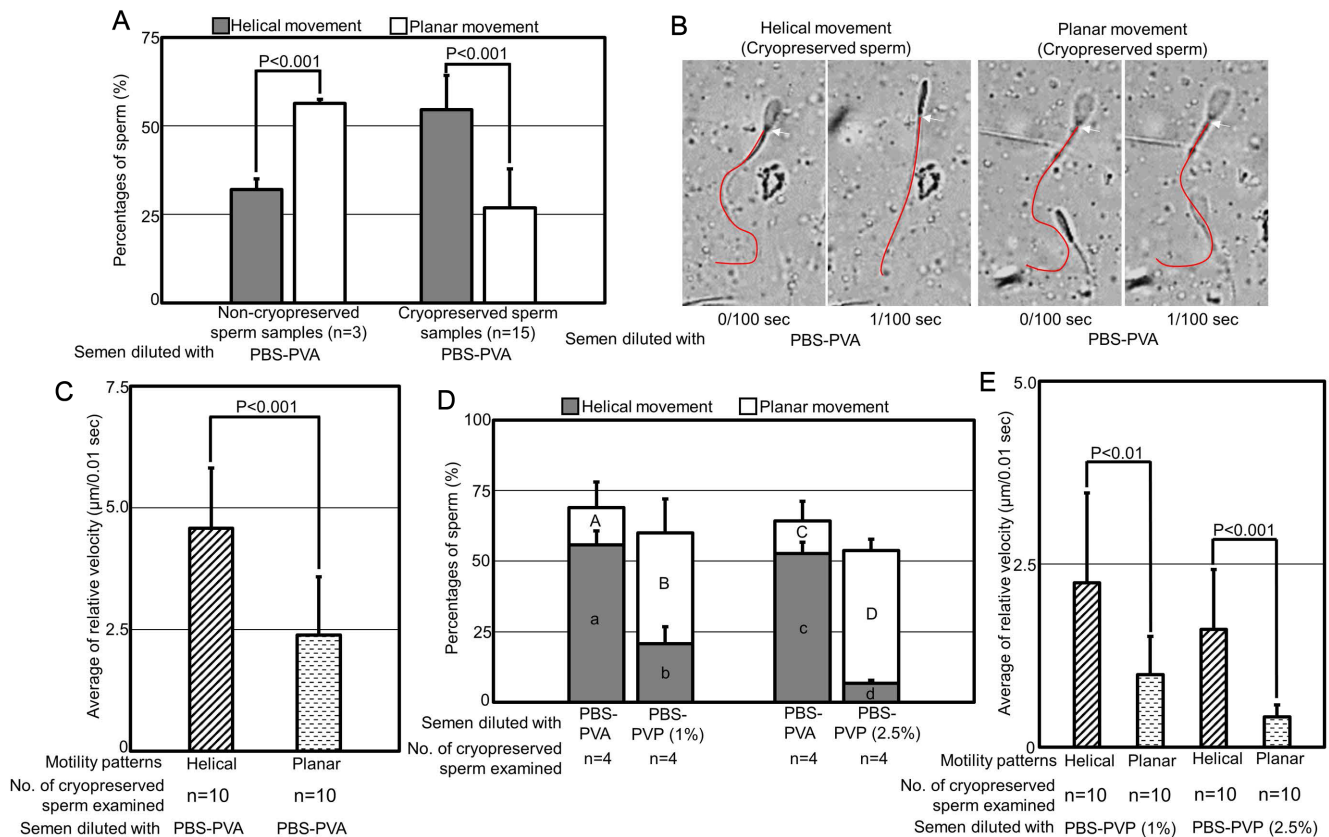
**Fig. 1.** Characteristics of motility of bovine cryopreserved spermatozoa. (A) Sperm motility patterns (helical movement and planar movement) of cryopreserved and non-cryopreserved semen which were diluted with phosphate-buffered saline containing 0.1% polyvinyl alcohol (PBS-PVA). (B) Typical examples of the microscopic images (two sequential frames which were captured at a frame rate of 100 Hz) of helically motile spermatozoa and planarly motile spermatozoa of the cryopreserved semen which was diluted with PBS-PVA; the flagellum of each spermatozoon (indicated with a white arrow) is highlighted with a red line to readily recognize its shape. (C) The average relative velocity of helically and planarly motile spermatozoa of the cryopreserved semen which was diluted with PBS-PVA. (D) Sperm motility patterns of cryopreserved semen which was diluted with phosphate-buffered saline containing 1 or 2.5% polyvinylpyrrolidone (PBS-PVP); values with different letters (A versus B, C versus D, a versus b, c versus d) are significantly different (P < 0.05). (E) The average relative velocity of helically and planarly motile spermatozoa of the cryopreserved semen which was diluted with PBS-PVP.

washing to remove the seminal plasma and egg yolk-based extender, both non-cryopreserved and cryopreserved spermatozoa maintained the same dominant patterns of movement in PBS-PVA (Fig. 2-A). These spermatozoa were used for the detection of cytoplasmic $Ca^{2+}$ in the flagella (Figs. 2-B, 2-C and Supplementary Fig. 3). The cryopreserved spermatozoa had large populations of live (PI-negative) cells with more intensive Fluo-3/AM fluorescence in the flagella (ranging from 151 to 350%), and the average relative intensity of Fluo-3/AM fluorescence (the average cytoplasmic $Ca^{2+}$ level) in the flagella was significantly higher in the cryopreserved spermatozoa than in the non-cryopreserved spermatozoa.

*Experiment 2. Involvement of SERCAs in suppressing the appearance of helically motile spermatozoa before cryopreservation*

We investigated the effects of thapsigargin on the motility patterns of non-cryopreserved spermatozoa incubated in non-capacitation medium containing 1.71 mM $CaCl_2$ (Fig. 3, Supplementary Movie 3 and Supplementary Fig. 2-C). In the control samples without thapsigargin before incubation, the percentages of helically motile and planarly motile spermatozoa were 26 ± 8% and 55 ± 5%, respectively. The addition of thapsigargin (10 μM) significantly decreased the planarly motile spermatozoa (39 ± 7%) even before

incubation, although after incubation for 45 min, the effects of thapsigargin (10 μM) were more pronounced. Specifically, treatment with thapsigargin (10 μM) induced helical movement with higher velocity and elevated cytoplasmic $Ca^{2+}$ levels in the flagella of non-cryopreserved spermatozoa. Non-cryopreserved spermatozoa with thapsigargin-induced helical movement were similar in terms of motility, flagellar bends, and cytoplasmic $Ca^{2+}$ levels in the flagella to the cryopreserved spermatozoa with helical movement.

To detect SERCAs in non-cryopreserved spermatozoa, we conducted Western blotting with a commercial antibody against SERCAs1/2/3. A broad band was observed on the blots around the molecular masses of 140 kDa (Fig. 4-A). This band resulted from this specific reaction because it was not detected in the negative control experiments that used normal mouse $IgG_1$ instead of the primary antibody. The broadness of this band may be explained by the possible mixture of at least two isoforms of the $Ca^{2+}$-ATPases with different molecular masses (the numbers of amino acids in the core polypeptides: bovine SERCA1 (accession XP_024840649.1), 1011 amino acids; bovine SERCA2 (accession XP_005217964.1), 997 amino acids; and bovine SERCA3 (accession XP_005220277.1), 1044 amino acids). However, the detection level of the SERCA band apparently decreased in the extracts from cryopreserved spermatozoa (Fig. 5, see additional information in the figure legend).
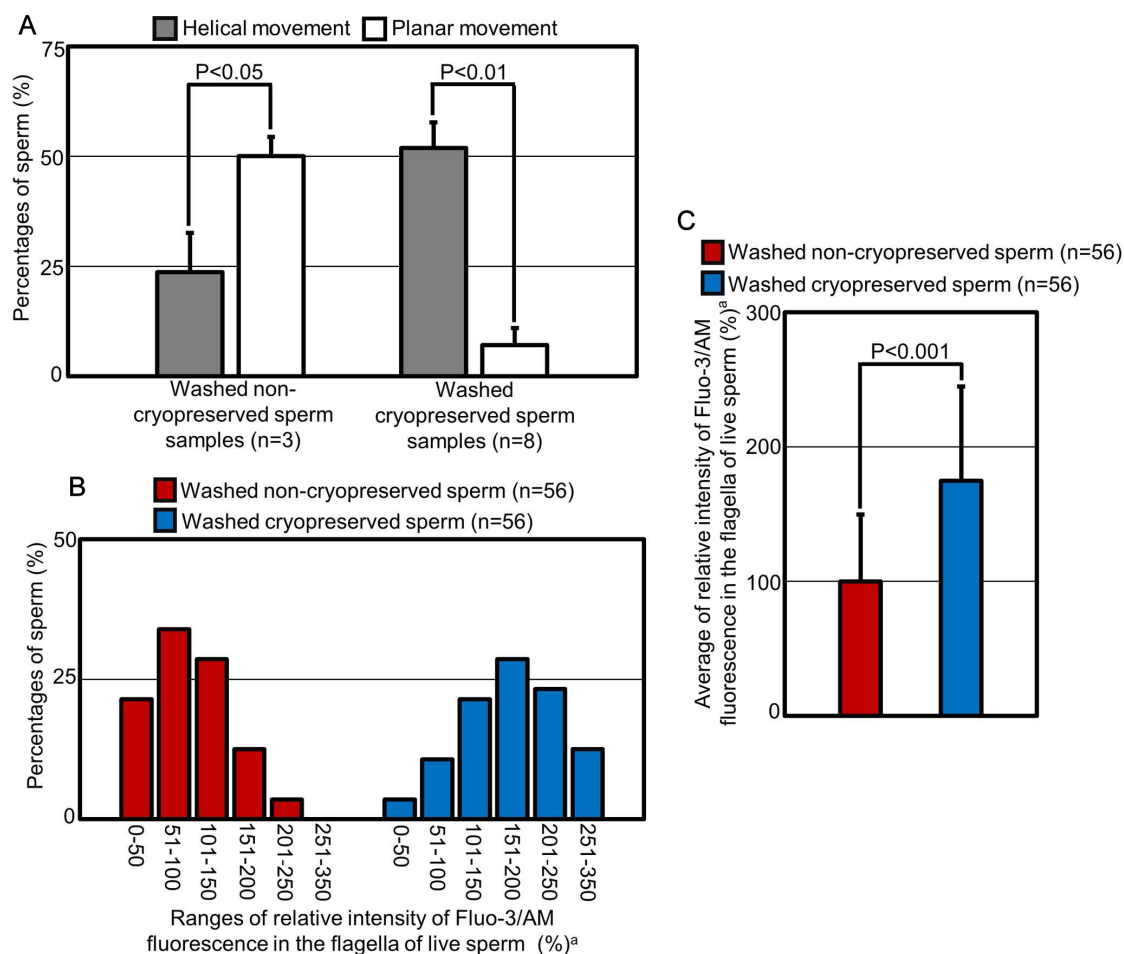
**Fig. 2.** Motility patterns and flagellar cytoplasmic $Ca^{2+}$ levels of bovine cryopreserved and non-cryopreserved spermatozoa which were washed with PBS-PVA. (A) Motility patterns, (B and C) Flagellar cytoplasmic $Ca^{2+}$ levels of live (propidium iodide (PI)-negative) spermatozoa; relative intensity of Fluo-3/AM fluorescence in the sperm flagellum was calculated according to the following formula. [a] Relative Fluo-3/AM fluorescence intensity in the flagellum of each live spermatozoon (%) = [(ImageJ value measured for each cryopreserved or non-cryopreserved live spermatozoon) ÷ (average of the ImageJ values measured for non-cryopreserved live spermatozoa)] × 100.

The localization of SERCAs in non-cryopreserved and cryopreserved spermatozoa was observed by indirect immunofluorescence. As shown in Fig. 4-B, and Supplementary Figs. 4 and 5, a clear fluorescent spot was visualized on one side of the neck (connecting piece) between the head and flagellum. No fluorescent signal was observed in the negative control experiments that used normal mouse $IgG_1$ instead of the primary antibody. In each of the four experiments for non-cryopreserved spermatozoa, 100 cells were examined at random to determine the side of the neck on which the fluorescent spot was. The percentage of spermatozoa with the fluorescent spot on the right side of the neck (51 ± 2%) was almost equal to that showing the spot on the left side (49 ± 2%), suggesting a unique (asymmetric) localization of SERCAs in bovine spermatozoa with a linearly symmetric shape.

*Experiment 3. Potential of helical movement to serve as an index of sperm quality*

There were large inter-bull differences in sperm motility patterns among the cryopreserved semen of the 10 Japanese Black bulls (Fig. 6-A). As shown in Fig. 6-B and Supplementary Fig. 6, the AI results (post-AI conception rates) had a significantly positive correlation with the percentage of spermatozoa exhibiting progressive/helical movement plus the percentage of spermatozoa exhibiting round/helical movement (i.e., the percentage of helically motile spermatozoa) (r = 0.806, P = 0.00486). However, they were not significantly correlated with the percentage of progressively motile spermatozoa (i.e., the percentage of spermatozoa exhibiting progressive/helical movement plus the percentage of spermatozoa exhibiting progressive/planar movement, r = 0.547, P = 0.102).

## Discussion

Bovine cryopreserved spermatozoa exhibit predominantly helical movement [9, 28], while vigorously motile spermatozoa with planar movement abound in non-cryopreserved semen [3]. The results of Experiment 1 confirmed these observations, and also suggest that bovine spermatozoa convert their motility pattern from planar to helical in response to cryopreservation-related changes. However, the mechanisms underlying the appearance of helical movement are poorly understood. According to our previous study [3], a reduction in cAMP signaling activity induced the conversion of motility patterns from planar to helical in bovine non-cryopreserved spermatozoa and coincidently decreased their velocity. However, the results of Experiment 1 showed that cryopreserved helically motile
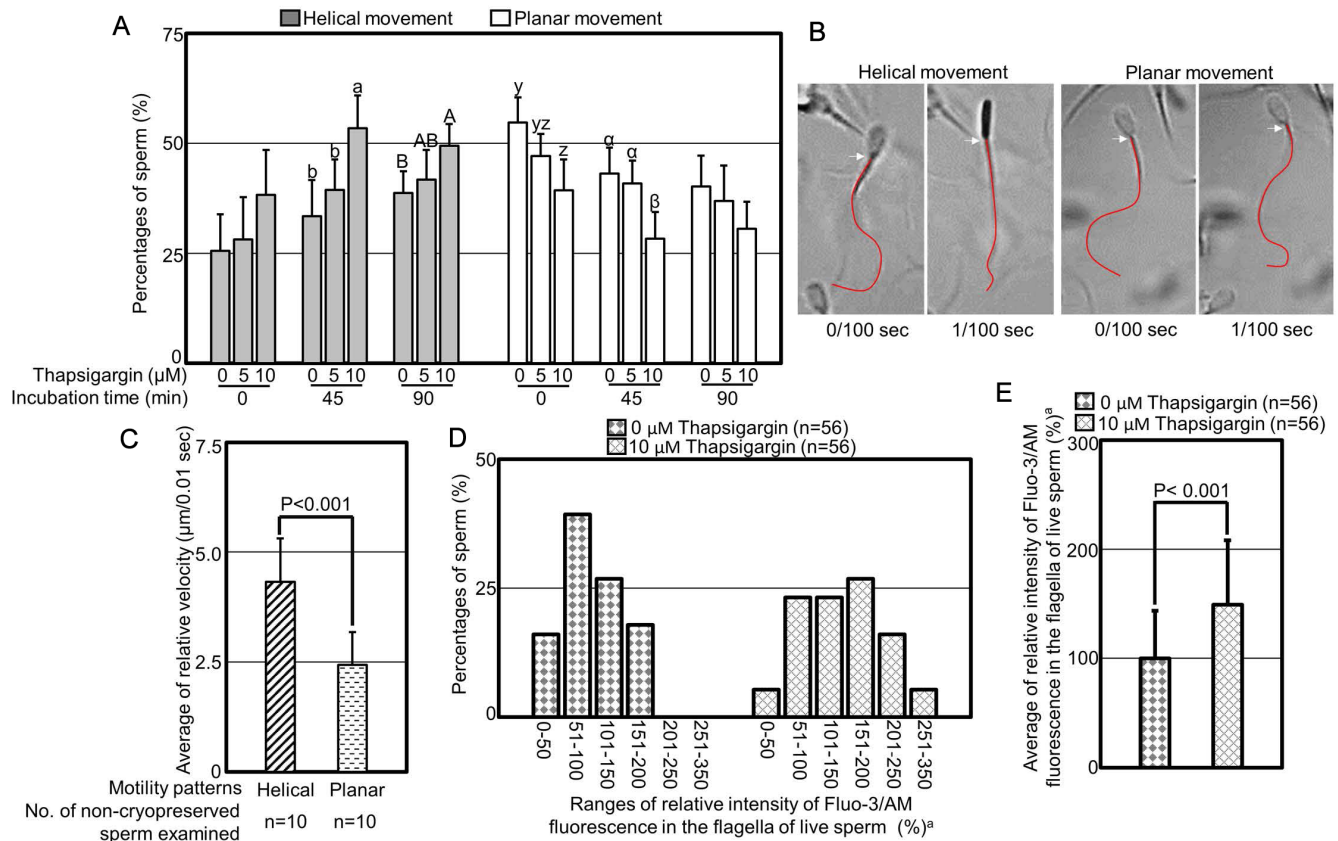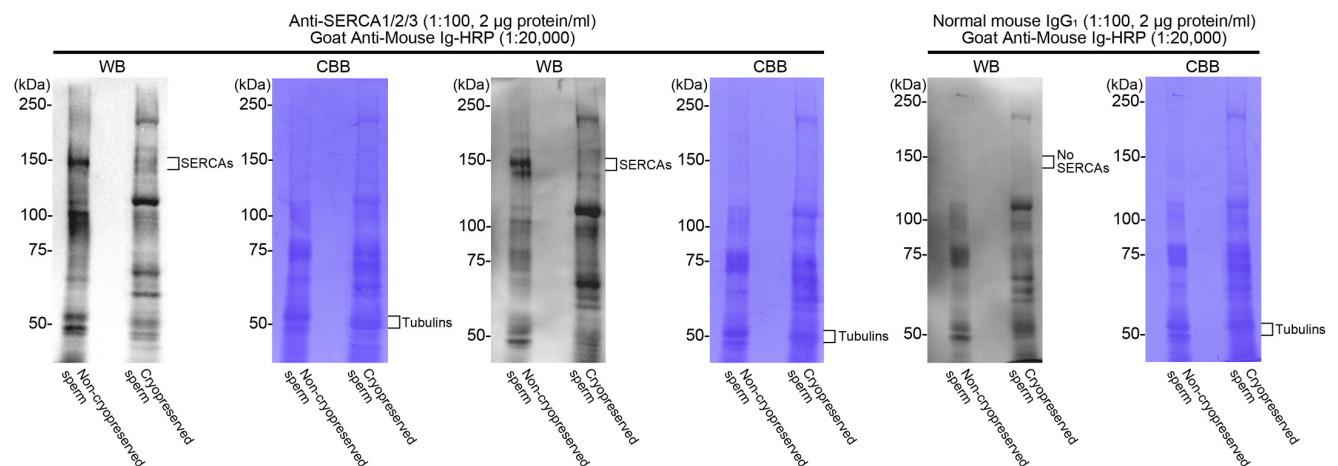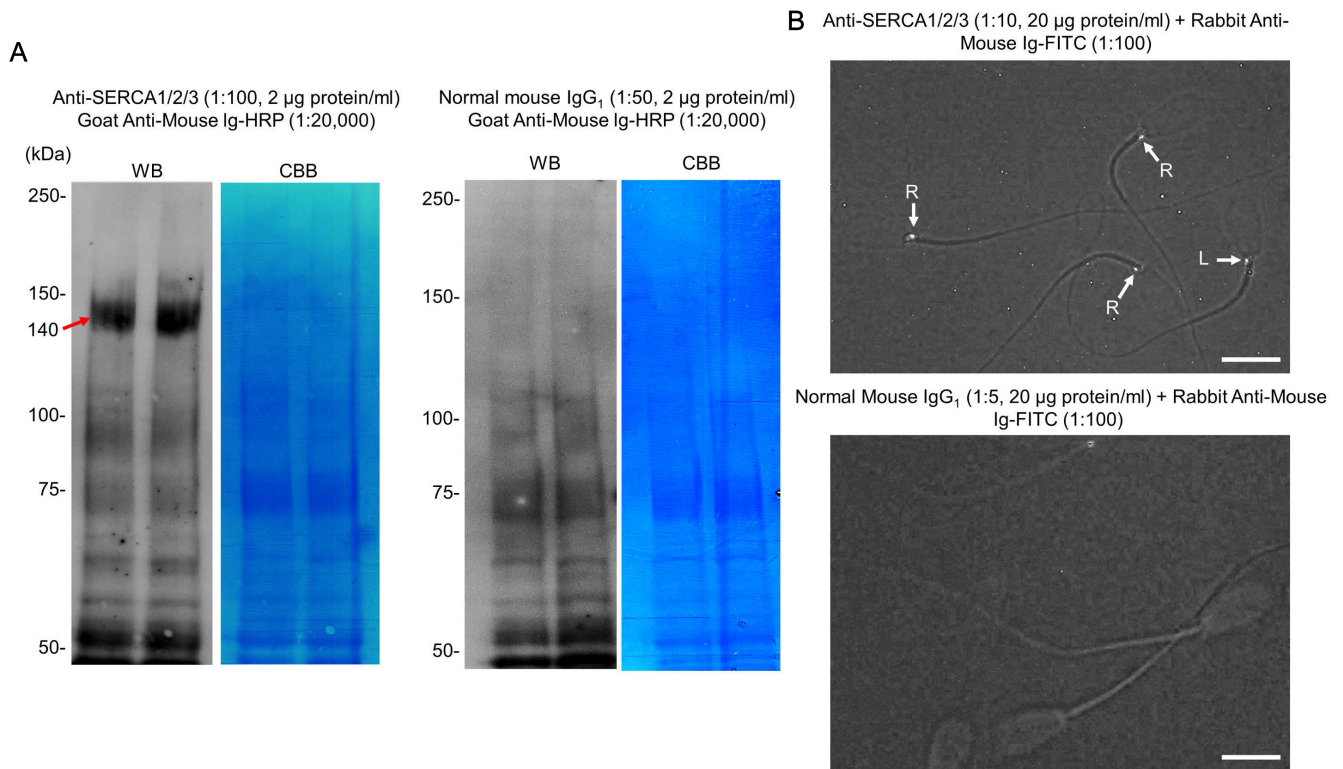
**Fig. 3.** Characteristics of motility and flagellar cytoplasmic $Ca^{2+}$ levels of bovine non-cryopreserved spermatozoa which were treated with an inhibitor for sarcoplasmic reticulum $Ca^{2+}$-ATPases (SERCAs). (A) Motility patterns of spermatozoa which were treated with thapsigargin; values with different letters (A *vs.* B, a *vs.* b, y *vs.* z, α *vs.* β) are significantly different (n = 7, P < 0.05). (B) Typical examples of the microscopic images (two sequential frames which were captured at a frame rate of 100 Hz) of helically motile spermatozoa and planarly motile spermatozoa which were treated with 10 μM thapsigargin for 45 min; the flagellum of each spermatozoon (indicated with a white arrow) is highlighted with a red line to readily recognize its shape. (C) The average relative velocity of non-cryopreserved helically motile spermatozoa and planarly motile spermatozoa which were treated with 10 μM thapsigargin for 45 min; (D and E) Flagellar cytoplasmic $Ca^{2+}$ levels of live (PI-negative) spermatozoa which were treated with or without 10 μM thapsigargin for 45 min; relative intensity of Fluo-3/AM fluorescence in the sperm flagellum was calculated according to the following formula. [a] Relative Fluo-3/AM fluorescence intensity in the flagellum of each live spermatozoon (%) = [(ImageJ value measured for each live spermatozoon treated with or without 10 μM thapsigargin for 45 min) ÷ (average of the ImageJ values measured for live spermatozoa treated without thapsigargin for 45 min)] × 100.

spermatozoa could produce a strong driving force and swim faster than cryopreserved planarly motile spermatozoa under both viscous and non-viscous conditions; moreover, the cytoplasmic $Ca^{2+}$ level of the flagella was significantly higher in the cryopreserved than in the non-cryopreserved spermatozoa. Thus, in Experiment 2, we focused on the cytoplasmic $Ca^{2+}$-dependent rather than the cAMP-dependent mechanism to investigate the factors underlying the appearance of helical movement in bovine spermatozoa.

Several reports have indicated that cryopreservation procedures increase cytoplasmic $Ca^{2+}$ levels of bovine spermatozoa [10–13]. Since SERCAs are important members of the cytoplasmic $Ca^{2+}$ clearance system and maintain intracellular $Ca^{2+}$ homeostasis of the spermatozoa [14], in Experiment 2, we examined the involvement of SERCAs in the appearance of helically motile spermatozoa. The results of the experiments showed that aspects of cryopreserved spermatozoa, such as the dominance of helical movement in the motility patterns, the higher velocity of helically motile spermatozoa, and the higher levels of cytoplasmic $Ca^{2+}$ in the flagella, could be mimicked by non-cryopreserved spermatozoa treated with thapsigargin. The localization of SERCAs in the sperm neck was also presented. The detection level of the SERCA band on Western blots apparently decreased in

spermatozoa after cryopreservation. As bovine spermatozoa possess an internal $Ca^{2+}$ store called the "redundant nuclear envelope" in the neck [22], it is reasonable to interpret that SERCAs of the neck pump cytoplasmic $Ca^{2+}$ into the redundant nuclear envelope and maintain a low $Ca^{2+}$ level in the sperm flagella. Thus, the results of Experiment 2 indicate that SERCAs of the neck play pivotal roles in suppressing the appearance of sperm helical movement before cryopreservation, and that cryopreservation procedures decrease sperm SERCAs, at least partially. Therefore, it is possible that the decrease in functional SERCAs elevates the cytoplasmic $Ca^{2+}$ level and consequently induces helical movement in cryopreserved bovine spermatozoa. However, we have not yet investigated the possible roles of other molecules in the intracellular $Ca^{2+}$ clearance system, specifically $Na^+$/$Ca^{2+}$ exchangers and plasma membrane $Ca^{2+}$-ATPases. Furthermore, previous reports indicate that the cryopreservation-related increase in sperm cytoplasmic $Ca^{2+}$ results from the permeation of extracellular $Ca^{2+}$ into the cytoplasm through the plasma membranes that change the lipid phase and fluidity [29, 30]. To determine the principal cause of the cryopreservation-related appearance of helically motile spermatozoa, it is necessary to conduct further experiments that compare the status of all molecules of the intracellular $Ca^{2+}$ clearance

**Fig. 4.** Immunodetection of SERCAs in bovine non-cryopreserved spermatozoa by Western blotting and indirect immunofluorescence. (A) Typical examples of Western blots (WB) of the extracts from the spermatozoa ($3 \times 10^6$ cells/lane) which were detected with the anti-SERCA1/2/3 antibody ($n = 5$) or normal mouse IgG$_1$ (Control, $n = 5$). After Western blotting, the major bands of sperm proteins were visualized by Coomassie brilliant blue (CBB, Quick-CBB PLUS of FUJIFILM Wako) staining. (B) Indirect immunofluorescence of the spermatozoa, which were detected with the anti-SERCA1/2/3 antibody ($n = 4$) or normal mouse IgG$_1$ (Control, $n = 4$). The images were taken under the blue fluorescence field with weak visible light and then converted to the gray-scale mode in order to clearly indicate the immunolocalization of the antigens. R: the spermatozoon with a fluorescence spot on the right-side edge of the neck, L: the spermatozoon with a fluorescence spot on the left-side edge of the neck. White bars indicate 10 μm.



**Fig. 5.** Comparison of immunodetection of SERCAs between bovine non-cryopreserved and cryopreserved spermatozoa by Western blotting. Representative examples of Western blots (WB) of the extracts from the spermatozoa ($3 \times 10^6$ cells/lane), which were detected with the anti-SERCA1/2/3 antibody ($n = 3$) or normal mouse IgG$_1$ (Control, $n = 1$). After Western blotting, the major bands of sperm proteins were visualized by Coomassie brilliant blue R-250 (CBB, Nacalai Tesque, Kyoto, Japan) staining. Additional information: When half the amount of the extracts from non-cryopreserved spermatozoa ($1.5 \times 10^6$ cells/lane) was used in Western blotting, the band of SERCAs was not detectable (data not shown). Thus, the faint detection of SERCAs in cryopreserved spermatozoa indicates that they include more than half of the antigen amount of non-cryopreserved spermatozoa.
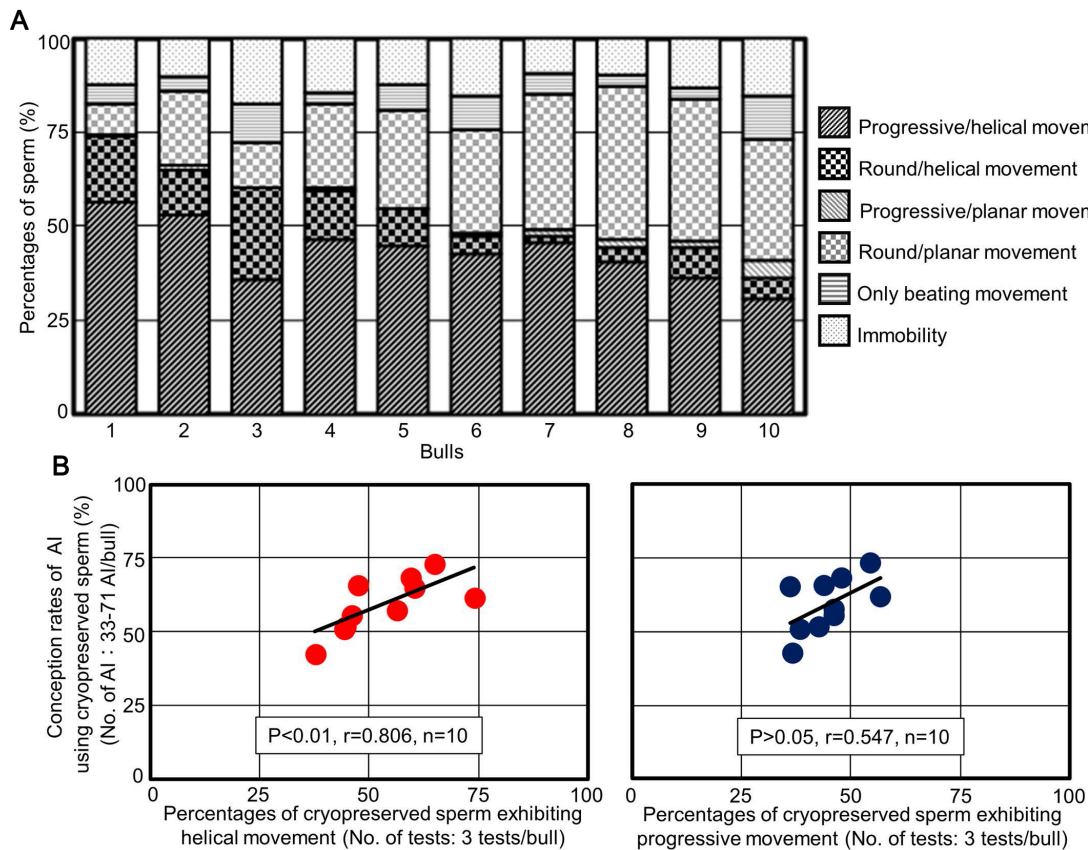
**Fig. 6.** Inter-bull differences in the motility patterns of bovine cryopreserved spermatozoa. (A) Sperm motility patterns (progressive/helical movement, round/helical movement, progressive/planar movement, round/planar movement, only beating movement and immobility) of cryopreserved semen which was diluted with PBS-PVA; Three examinations were performed for each bull. (B) Correlation of the results of artificial insemination (AI) (conception rates of AI using cryopreserved sperm) with percentages of cryopreserved spermatozoa exhibiting helical movement (percentages of spermatozoa exhibiting progressive/helical movement + percentages of spermatozoa exhibiting round/helical movement) or percentages of cryopreserved spermatozoa exhibiting progressive movement (percentages of spermatozoa exhibiting progressive/helical movement + percentages of spermatozoa exhibiting progressive/planar movement); each symbol in the graphs indicates the results for each bull.

system and the $Ca^{2+}$ permeability of plasma membranes between non-cryopreserved and cryopreserved spermatozoa.

In this study, Western blotting and indirect immunofluorescence (Experiment 2) showed a unique distribution of SERCAs in either the right or left edge of the neck (connecting piece) of the bovine spermatozoon with a linearly symmetric shape. Another study also indicated the asymmetry of subcellular localization of the motility regulator (the voltage-gated proton channel Hv1 of human sperm flagella). This channel is important in the occurrence of flagellar rotation (which is likely the same as helical movement) and subsequent hyperactivation [31]. These results indicate the existence of intracellular $Ca^{2+}$ level modulators that are localized asymmetrically in spermatozoa with a linearly symmetric shape.

To reach the ampulla of the oviduct and then penetrate the oocyte-cumulus complex, mammalian ejaculated spermatozoa need to be transported through the uterus and oviduct, which contain luminal fluid with complex physical properties. However, in these reproductive tracts, several barriers limit sperm passage and arrest poor-quality spermatozoa. For example, the cervical mucus acts as a gatekeeper to exclude aberrant and weakly motile/immotile spermatozoa; thus, progressive movement may be required for successful cervical penetration [32–35]. The isthmus of the oviduct, including the uterotubal junction, is a narrow cascade containing luminal mucus [36], and transportation through this section is modulated by both

sperm motility and oviductal factors including myosalpinx contraction and oviduct fluid flow [37, 38]. It is generally considered that hyperactivated movement is important for sperm passage through the isthmus and subsequent penetration into the oocyte-cumulus complexes in the ampulla of the oviduct [39–41]. In bovine AI, as cryopreserved spermatozoa are inseminated directly into the corpus uterus, their first requirement in order to accomplish fertilization is to pass through the isthmus of the oviduct, including the uterotubal junction. As observed in Experiments 1 and 2 and in our previous studies [5, 39], the helical movement (see Supplementary Movies 1 and 3) apparently differed from hyperactivation in both the trajectory of motion and the flagellar beating patterns (see Supplementary Movies in [39] https://www.ncbi.nlm.nih.gov/pmc/articles/PMC6194283/bin/RMB2-17-442-s001.mp4), although both of these motility patterns appeared with an increase in cytoplasmic $Ca^{2+}$. We also observed that a limited number of cryopreserved spermatozoa maintained helical movement and showed stronger driving forces in the viscous medium containing PVP than the planarly motile spermatozoa (Experiment 1). The AI results (post-AI conception rates) were significantly positively correlated with the percentage of cryopreserved, helically motile spermatozoa (r = 0.806, P = 0.00486) (Experiment 3). These observations indicate that helically motile spermatozoa of AI-used cryopreserved semen have a greater chance of fertilizing oocytes in the ampulla of the oviduct. This may be supported by our suggestion

that not only hyperactivation but also helical movement are beneficial to sperm passage through the isthmus of the oviduct.

Previous studies have shown the importance of investigating changes in acrosome morphology during incubation in the capacitation-supporting medium to determine the quality of bovine cryopreserved spermatozoa, because cryo-capacitation promotes the precocious acrosome reaction by the earlier elevation of the cytoplasmic $Ca^{2+}$ level and has deleterious effects on AI results [13, 42, 43]. In addition to these facts, we proposed here that it is necessary to focus on the benefits of the cryo-capacitation-related appearance of helical movement to improve the examination of bovine cryopreserved semen, because the results of Experiment 3 indicate the potential of sperm helical movement as a positive parameter to predict the results of AI using cryopreserved semen.

**Conflict of interests:** The authors declare no conflict of interest.

## Acknowledgement

## References

1. **Kathiravan P, Kalatharan J, Karthikeya G, Rengarajan K, Kadirvel G.** Objective sperm motion analysis to assess dairy bull fertility using computer-aided system—a review. *Reprod Domest Anim* 2011; **46**: 165–172. [Medline] [CrossRef]

2. **Amann RP, Waberski D.** Computer-assisted sperm analysis (CASA): capabilities and potential developments. *Theriogenology* 2014; **81**: 5–17.e1: 3. [Medline] [CrossRef]

3. **Yamada A, Sakase M, Fukushima M, Harayama H.** Reconsideration of the evaluation criteria for bull ejaculated sperm motility in the context of rotation. *J Reprod Dev* 2018; **64**: 377–384. [Medline] [CrossRef]

4. **Arai Y, Sakase M, Fukushima M, Harayama H.** Identification of isoforms of calyculin A-sensitive protein phosphatases which suppress full-type hyperactivation in bull ejaculated spermatozoa. *Theriogenology* 2019; **129**: 46–53. [Medline] [CrossRef]

5. **Saha SR, Sakase M, Fukushima M, Harayama H.** Effects of digoxin on full-type hyperactivation in bovine ejaculated spermatozoa with relatively lower survivability for incubation with stimulators of cAMP signaling cascades. *Theriogenology* 2020; **154**: 100–109. [Medline] [CrossRef]

6. **Soler C, Picazo-Bueno JÁ, Micó V, Valverde A, Bompart D, Blasco FJ, Álvarez JG, García-Molina A.** Effect of counting chamber depth on the accuracy of lensless microscopy for the assessment of boar sperm motility. *Reprod Fertil Dev* 2018; **30**: 924–934. [Medline] [CrossRef]

7. **Roldan ERS.** Assessments of sperm quality integrating morphology, swimming patterns, bioenergetics and cell signalling. *Theriogenology* 2020; **150**: 388–395. [Medline] [CrossRef]

8. **van der Horst G.** Computer Aided Sperm Analysis (CASA) in domestic animals: Current status, three D tracking and flagellar analysis. *Anim Reprod Sci* 2020; **220**: 106350. [Medline] [CrossRef]

9. **Ishijima S, Hamaguchi MS, Naruse M, Ishijima SA, Hamaguchi Y.** Rotational movement of a spermatozoon around its long axis. *J Exp Biol* 1992; **163**: 15–31. [Medline] [CrossRef]

10. **Bailey JL, Buhr MM.** Regulation of internal $Ca^{2+}$ by chilled bull and boar spermatozoa. *Cryobiology* 1995; **32**: 259–269. [Medline] [CrossRef]

11. **Cormier N, Sirard M-A, Bailey JL.** Premature capacitation of bovine spermatozoa is initiated by cryopreservation. *J Androl* 1997; **18**: 461–468. [Medline]

12. **Cormier N, Bailey JL.** A differential mechanism is involved during heparin- and cryopreservation-induced capacitation of bovine spermatozoa. *Biol Reprod* 2003; **69**: 177–185. [Medline] [CrossRef]

13. **Pons-Rejraji H, Bailey JL, Leclerc P.** Cryopreservation affects bovine sperm intracellular parameters associated with capacitation and acrosome exocytosis. *Reprod Fertil Dev* 2009; **21**: 525–537. [Medline] [CrossRef]

14. **Olson SD, Fauci LJ, Suarez SS.** Mathematical modeling of calcium signaling during sperm hyperactivation. *Mol Hum Reprod* 2011; **17**: 500–510. [Medline] [CrossRef]

15. **Chemaly ER, Troncone L, Lebeche D.** SERCA control of cell death and survival. *Cell Calcium* 2018; **69**: 46–61. [Medline] [CrossRef]

16. **Kishida K, Sakase M, Minami K, Arai MM, Syoji R, Kohama N, Akiyama T, Oka A,**

17. **Harayama H, Fukushima M.** Effects of acrosomal conditions of frozen-thawed spermatozoa on the results of artificial insemination in Japanese Black cattle. *J Reprod Dev* 2015; **61**: 519–524. [Medline] [CrossRef]

18. **Mizuno Y, Isono A, Kojima A, Arai MM, Noda T, Sakase M, Fukushima M, Harayama H.** Distinct segment-specific functions of calyculin A-sensitive protein phosphatases in the regulation of cAMP-triggered events in ejaculated bull spermatozoa. *Mol Reprod Dev* 2015; **82**: 232–250. [Medline] [CrossRef]

18. **Harayama H, Sasaki K, Miyake M.** A unique mechanism for cyclic adenosine 3′,5′-monophosphate-induced increase of 32-kDa tyrosine-phosphorylated protein in boar spermatozoa. *Mol Reprod Dev* 2004; **69**: 194–204. [Medline] [CrossRef]

19. **Barritt GJ.** Does a decrease in subplasmalemmal $Ca^{2+}$ explain how store-operated $Ca^{2+}$ channels are opened? *Cell Calcium* 1998; **23**: 65–75. [Medline] [CrossRef]

20. **Inesi G, Hua S, Xu C, Ma H, Seth M, Prasad AM, Sumbilla C.** Studies of $Ca^{2+}$ ATPase (SERCA) inhibition. *J Bioenerg Biomembr* 2005; **37**: 365–368. [Medline] [CrossRef]

21. **Salido GM, Sage SO, Rosado JA.** TRPC channels and store-operated $Ca^{2+}$ entry. *Biochim Biophys Acta* 2009; **1793**: 223–230. [Medline] [CrossRef]

22. **Ho H-C, Suarez SS.** An inositol 1,4,5-trisphosphate receptor-gated intracellular $Ca^{2+}$ store is involved in regulating sperm hyperactivated motility. *Biol Reprod* 2001; **65**: 1606–1615. [Medline] [CrossRef]

23. **Jimenez-Gonzalez C, Michelangeli F, Harper CV, Barratt CL, Publicover SJ.** Calcium signalling in human spermatozoa: a specialized 'toolkit' of channels, transporters and stores. *Hum Reprod Update* 2006; **12**: 253–267. [Medline] [CrossRef]

24. **Harayama H, Noda T, Ishikawa S, Shidara O.** Relationship between cyclic AMP-dependent protein tyrosine phosphorylation and extracellular calcium during hyperactivation of boar spermatozoa. *Mol Reprod Dev* 2012; **79**: 727–739. [Medline] [CrossRef]

25. **Harayama H, Miyake M.** A cyclic adenosine 3′,5′-monophosphate-dependent protein kinase C activation is involved in the hyperactivation of boar spermatozoa. *Mol Reprod Dev* 2006; **73**: 1169–1178. [Medline] [CrossRef]

26. **Wada A, Harayama H.** Calmodulin is involved in the occurrence of extracellular $Ca^{2+}$-dependent full-type hyperactivation in boar ejaculated spermatozoa incubated with cyclic AMP analogs. *Anim Sci J* 2021; **92**: e13552. [Medline] [CrossRef]

27. **Kojima A, Matsushita Y, Ogura Y, Ishikawa S, Noda T, Murase T, Harayama H.** Roles of extracellular $Ca^{2+}$ in the occurrence of full-type hyperactivation in boar ejaculated spermatozoa pre-incubated to induce the cAMP-triggered events. *Andrology* 2015; **3**: 321–331. [Medline] [CrossRef]

28. **Nosrati R, Driouchi A, Yip CM, Sinton D.** Two-dimensional slither swimming of sperm within a micrometre of a surface. *Nat Commun* 2015; **6**: 8703. [Medline] [CrossRef]

29. **Bailey J, Buhr M.** Cryopreservation alters the $Ca^{2+}$ flux of bovine spermatozoa. *Can J Anim Sci* 1994; **74**: 45–51. [CrossRef]

30. **Collin S, Sirard MA, Dufour M, Bailey JL.** Sperm calcium levels and chlortetracycline fluorescence patterns are related to the in vivo fertility of cryopreserved bovine semen. *J Androl* 2000; **21**: 938–943. [Medline]

31. **Miller MR, Kenny SJ, Mannowetz N, Mansell SA, Wojcik M, Mendoza S, Zucker RS, Xu K, Lishko PV.** Asymmetrically positioned flagellar control units regulate human sperm rotation. *Cell Reports* 2018; **24**: 2606–2613. [Medline] [CrossRef]

32. **Aitken RJ, Sutton M, Warner P, Richardson DW.** Relationship between the movement characteristics of human spermatozoa and their ability to penetrate cervical mucus and zona-free hamster oocytes. *J Reprod Fertil* 1985; **73**: 441–449. [Medline] [CrossRef]

33. **Mortimer D, Pandya IJ, Sawers RS.** Relationship between human sperm motility characteristics and sperm penetration into human cervical mucus in vitro. *J Reprod Fertil* 1986; **78**: 93–102. [Medline] [CrossRef]

34. **Murase T, Okuda K, Sato K.** Assessment of bull fertility using a mucus penetration test and a human chorionic gonadotrophin stimulation test. *Theriogenology* 1990; **34**: 801–812. [Medline] [CrossRef]

35. **Martyn F, McAuliffe FM, Wingfield M.** The role of the cervix in fertility: is it time for a reappraisal? *Hum Reprod* 2014; **29**: 2092–2098. [Medline] [CrossRef]

36. **Suarez SS, Brockman K, Lefebvre R.** Distribution of mucus and sperm in bovine oviducts after artificial insemination: the physical environment of the oviductal sperm reservoir. *Biol Reprod* 1997; **56**: 447–453. [Medline] [CrossRef]

37. **Ishikawa Y, Usui T, Yamashita M, Kanemori Y, Baba T.** Surfing and swimming of ejaculated sperm in the mouse oviduct. *Biol Reprod* 2016; **94**: 89. [Medline] [CrossRef]

38. **Hino T, Yanagimachi R.** Active peristaltic movements and fluid production of the mouse oviduct: their roles in fluid and sperm transport and fertilization. *Biol Reprod* 2019; **101**: 40–49. [Medline] [CrossRef]

39. **Harayama H.** Flagellar hyperactivation of bull and boar spermatozoa. *Reprod Med Biol* 2018; **17**: 442–448. [Medline] [CrossRef]

40. **Suarez SS, Dai X.** Hyperactivation enhances mouse sperm capacity for penetrating viscoelastic media. *Biol Reprod* 1992; **46**: 686–691. [Medline] [CrossRef]

41. **Chang H, Suarez SS.** Unexpected flagellar movement patterns and epithelial binding behavior of mouse sperm in the oviduct. *Biol Reprod* 2012; **86**: 140: 1–8. [Medline] [CrossRef]

42. **Bailey JL, Bilodeau JF, Cormier N.** Semen cryopreservation in domestic animals: a damaging and capacitating phenomenon. *J Androl* 2000; **21**: 1–7. [Medline]

43. **Kuroda K, Fukushima M, Harayama H.** Premature capacitation of frozen-thawed spermatozoa from subfertile Japanese black cattle. *J Reprod Dev* 2007; **53**: 1079–1086. [Medline] [CrossRef]